Field tuning of domain-wall type and chirality in $SrRuO_3$

Debangsu Roy,[1] Sagi Davidovitch,[2] Yu-Ming Hung,[1] Moty Schultz,[2] Stephen D. Albright,[3] M. D. Morales-Acosta,[4] Frederick J. Walker,[4] James W. Reiner,[5] C. H. Ahn,[4] Andrew D. Kent,[1] and Lior Klein[2]

[1]*Department of Physics, New York University, New York, New York 10003, USA*

[2]*Department of Physics, Nano-magnetism Research Center, Institute of Nanotechnology and Advanced Materials, Bar-Ilan University, Ramat-Gan 52900, Israel*

[3]*Department of Physics, Yale University, New Haven, Connecticut 06520, USA*

[4]*Department of Applied Physics, Yale University, New Haven, Connecticut 06520, USA*

[5]*HGST, a Western Digital Company, San Jose, California 95135, USA*

(Received 8 February 2017; revised manuscript received 5 May 2017; published 30 June 2017)

$SrRuO_3$ films have large uniaxial magnetocrystalline anisotropy tilted out of the film plane. When cooled in zero field from above the Curie temperature (∼150 K), a magnetic domain structure emerges in the form of 200-nm-wide stripes oriented along the in-plane projection of the magnetic easy axis. We measure the interface resistance of the magnetic domain walls by applying a magnetic field perpendicular to the easy axis in the domain-wall plane and perpendicular to this plane and observe hysteretic behavior. Micromagnetic simulations of the results indicate that, depending on the direction in which the field is applied, the domain-wall type (Bloch or Néel) and chirality can be tuned.

DOI: 10.1103/PhysRevB.95.224437

I. INTRODUCTION

Ferromagnetic materials tend to subdivide into multiple magnetic domains in zero field to reduce their magnetostatic energy [1,2]. The interface between neighboring domains is called a domain wall (DW) and in it the magnetization gradually rotates across a distance called the DW width. Although DWs have been observed and studied for decades, the emergence of spintronics has attracted new interest in DWs, particularly in their interactions with spin-transfer [3] and spin-orbit torques, and for their importance in the development of novel spintronic devices, including for advanced data storage and logic processing [4,5].

DWs in ferromagnetic materials with uniaxial magnetic anisotropy are commonly either Bloch or Néel walls. In both cases the rotation axis of the magnetization in the DW is perpendicular to the easy axis of magnetization: for a Bloch wall the axis is perpendicular to the DW plane, whereas for a Néel wall it is in the DW plane. Generally, Bloch walls are expected in ferromagnetic films with perpendicular magnetic anisotropy, whereas Néel walls are expected for films with in-plane magnetic anisotropy. Intermediate types of walls can also occur. In such a case, the rotation axis is expected to be in-between the rotation axes of Néel and Bloch walls in the plane defined by the two axes. The structure of the DW has a profound effect on its behavior in the presence of spin-transfer and spin-orbit torques, which makes the elucidation of the DW structure particularly important.

DWs in the itinerant ferromagnet $SrRuO_3$ have played a significant role in studying the interactions between DWs and current. The DWs are in the form of stripes which are ∼200 nm wide and the estimated DW width is ∼3 nm [6]. Previous studies have demonstrated large interface resistance and indicated that the same physical mechanism is pertinent to domain-wall resistivity (DWR) in $SrRuO_3$ and to the resistance of magnetic multilayers [7]. In particular, the DWR with perpendicular current matches with the resistivity induced by two sources relevant to magnetic multilayers; namely, spin accumulation and potential step [8]. In addition, efficient current-induced DW motion has been demonstrated [9].

Here, we study magnetic-field-induced changes of DW structure in $SrRuO_3$ with the field applied perpendicularly to the easy axis of the magnetization, by monitoring changes in the DW interface resistance. The perpendicular field is applied in the DW plane and perpendicular to this plane. To extract changes in the DWR, we compare the magnetoresistance (MR) of our samples with and without DWs. This is quite challenging in view of the fact that the contribution of the interface resistance to the total measured resistance is less than ten percent and the domain themselves exhibit their own MR. For this reason it is crucial that the field is aligned as much as possible perpendicularly to the easy axis to avoid changes in the location and number of the DWs. As we show below, these goals were indeed achieved.

We find that the high-field MR is negative and we associate this behavior with the decrease in the overall angular change in the magnetic-moment orientation across the DW. At low fields the MR is hysteretic. Supported by numerical simulations, the low-field results indicate that, when a field is applied in the DW plane, a Bloch wall is stabilized; whereas when a field is applied perpendicular to the DW plane, a Néel wall is stabilized. Moreover, the chirality of both walls is also tuned by the field and is responsible for the hysteretic behavior. The remarkable features of DWs in $SrRuO_3$ are of particular importance because they open new routes for studying the role of domain-wall structure in determining the interaction of DWs with spin-transfer and spin-orbit torques.

II. EXPERIMENTAL DETAILS

Our samples are epitaxial $SrRuO_3$ thin films grown on slightly miscut (∼2°) substrates of $SrTiO_3$ by reactive electron-beam evaporation. Growth techniques followed closely those previously documented [10]. The measurements were performed on films of different thicknesses (20 and 90 nm), which

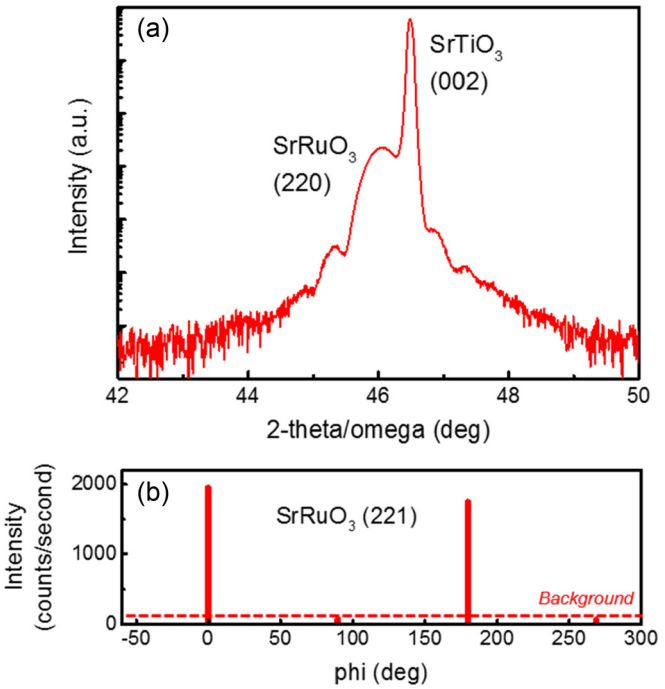

FIG. 1. (a) X-ray diffraction near the $SrTiO_3$ (002) and $SrRuO_3$ (220) reflections. (b) Intensity of omega rocking curves measured at $SrRuO_3$ (221) diffraction peaks at in-plane angles varying by 90°. The twofold symmetry of $SrRuO_3$ (221) peaks indicate that the film does not contain twinned domains.

exhibit similar behavior. The measurements of the 20-nm-thick film are presented. The crystal structure of 20 nm $SrRuO_3$ films was determined by x-ray diffraction using a monochromatic Rigaku Smartlab system. A diffraction peak corresponding to the $SrRuO_3$ (220) reflection is observed near the $SrTiO_3$ (002) reflection [Fig. 1(a)], demonstrating oriented growth of $SrRuO_3$ (110) plane on the (001) surface of $SrTiO_3$. Sharp rocking curves measured at the $SrRuO_3$ diffraction peaks, with full width at half maximum values less than 0.1°, indicate high crystalline order of the $SrRuO_3$ thin films. Orthorhombic lattice parameters of $a \cong 5.53$, $b \cong 5.57$, and $c \cong 7.85$ Å are extracted from the position of the $SrRuO_3$ (220) and (221) peaks, shown in Fig. 1. Peaks corresponding to the (221) reflection of $SrRuO_3$ are only observed at two in-plane angles differing by 180° [Fig. 1(b)], demonstrating that $SrRuO_3$ films are untwinned on miscut $SrTiO_3$ substrates. Miscut $SrTiO_3$ has previously been shown to remove twinning in $SrRuO_3$ growth [11].

The films are untwinned orthorhombic single crystals with lattice parameters of $a \cong 5.53$, $b \cong 5.57$, and $c \cong 7.85$ Å. The Curie temperature T_C of these films is ∼150 K and they exhibit an intrinsic uniaxial magnetocrystalline anisotropy where the anisotropy field in the low-temperature limit is more than ∼7 T [12]. The easy axis varies in the (001) plane between 45° from the film normal at T_C to 30° in the low-temperature limit (2 K) [13]. The large uniaxial anisotropy induces a stripe domain structure of width of ∼200 nm and narrow domain walls (∼3 nm). The samples are patterned by using e-beam lithography and Ar^+ ion milling for transverse and longitudinal resistivity measurements carried out in Quantum Design PPMS-9 (see inset in Fig. 2).

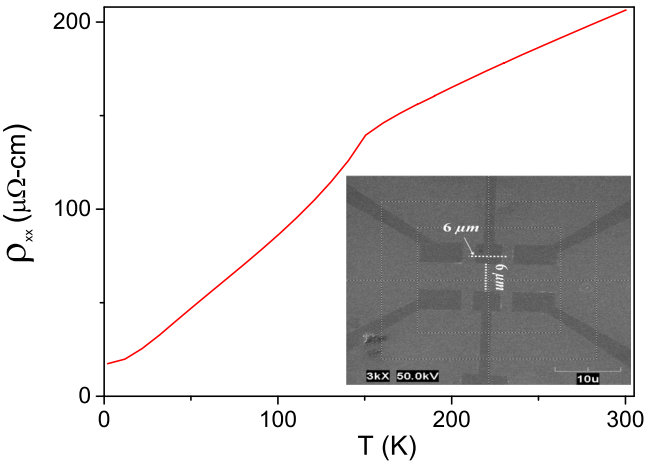

FIG. 2. ρ_{xx} vs temperature. Inset depicts the typical geometry of the samples.

III. EXPERIMENTAL RESULTS

Figure 2 presents the temperature dependence of the longitudinal resistivity ρ_{xx} of the film whose measurements are presented in the following figures. We note the resistivity ratio (∼12) which reflects its high quality. The effect of DWs on the resistivity is determined by comparing resistivities with and without DWs, which we denote by ρ_{xx}^{DWs} and $\rho_{xx}^{\mathrm{NDWs}}$, respectively. The domain state is obtained by zero-field cooling from above T_C. The state with no DWs can be obtained by applying a sufficiently large magnetic field along the easy axis. When the field is set back to zero, a uniformly magnetized remanent state is obtained. We define the DWR as the difference between ρ_{xx}^{DWs} and $\rho_{xx}^{\mathrm{NDWs}}$. Since the DWR depends on the angle between the current and the wall, we distinguish between DWR with current perpendicular or parallel to the DWs, which we denote as $\rho_{\mathrm{DW}}^{\perp}$ and $\rho_{\mathrm{DW}}^{\parallel}$, respectively.

We explore field-induced changes in the DW structure by using three different configurations. In the first two configurations, the magnetic field is applied along the [001] direction (perpendicular to the DW plane). In configuration 1 the current is parallel to the field [see inset of Fig. 3(b)]. In configuration 2 the current is perpendicular to the field [see inset of Fig. 4(b)]. In configuration 3 the field is applied along the hard axis in the (001) plane and the current is applied in the [001] direction [see inset in Fig. 5].

We start by presenting measurements in configuration 1 and 2. Figure 3 shows MR measurements of ρ_{xx}^{DWs}, $\rho_{xx}^{\mathrm{NDWs}}$, and $\rho_{\mathrm{DW}}^{\perp}$ in configuration 1. Figure 4 shows MR measurements of ρ_{xx}^{DWs}, $\rho_{xx}^{\mathrm{NDWs}}$, and $\rho_{\mathrm{DW}}^{\parallel}$ in configuration 2. In both cases $\rho_{xx}^{\mathrm{NDWs}}$ is reversible whereas ρ_{xx}^{DWs} is hysteretic. Also, despite qualitative differences in the behavior of ρ_{xx}^{DWs}, $\rho_{\mathrm{DW}}^{\perp}$ and $\rho_{\mathrm{DW}}^{\parallel}$ are qualitatively similar. We note that $\rho_{xx}^{\mathrm{NDWs}}$ exhibits some field asymmetry which can be attributed to a small deviation from the [001] direction which is within the angular resolution of our rotator (2°). No asymmetry is observed in the domain state since the asymmetry for the two types of domains is reversed; therefore, it is averaged out. In extracting the DWR, the asymmetric measurements were symmetrized. Additionally we found the difference in the resistivity value at zero field

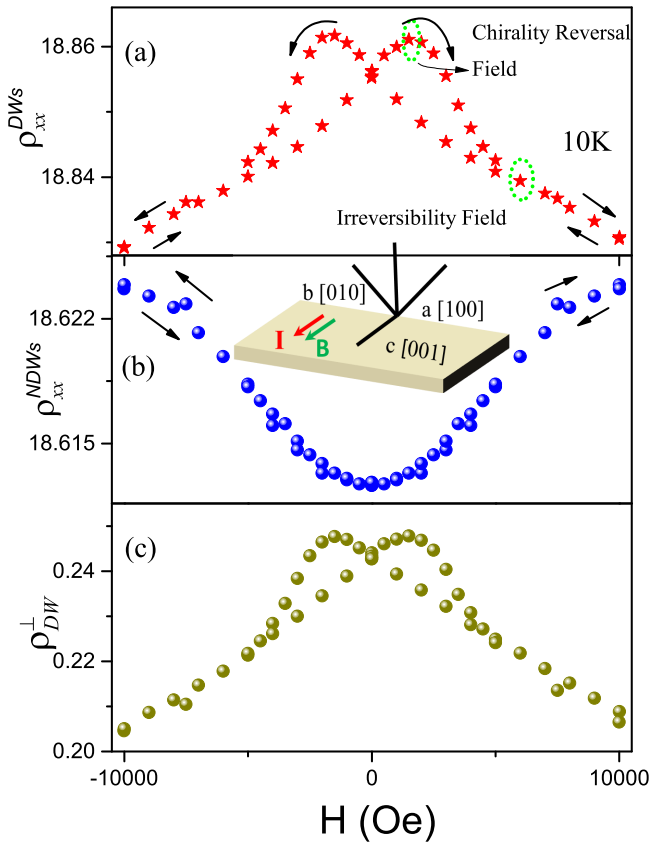

FIG. 3. (a) ρ_{xx} vs H when the sample is in a domain state. The field is applied along the [001] direction with current flowing perpendicular to the DWs at 10 K. The arrows indicate the field-sweeping direction. (b) ρ_{xx} vs H when the sample is uniformly magnetized. The field is applied along the [001] direction with current flowing perpendicular to the DWs at 10 K. The arrows indicate the field-sweeping direction. (c) MR of the DW at 10 K with the field applied along the [001] direction with current perpendicular to the DWs. All units are in $\mu\Omega$ cm.

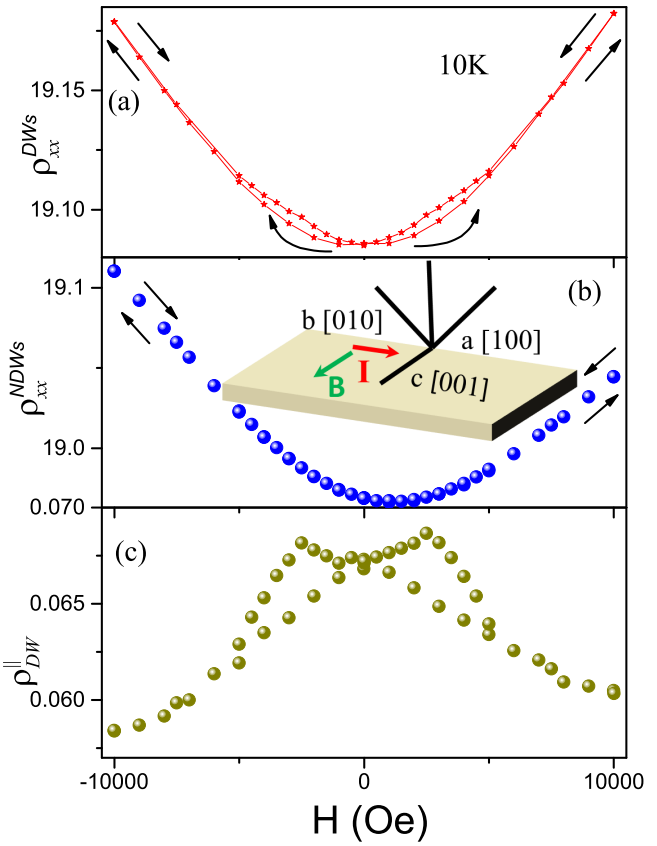

FIG. 4. (a) ρ_{xx} vs H when the sample is in a domain state. The field is applied along the [001] direction with current flowing parallel to the DWs at 10 K. The arrows indicate the field-sweeping direction. (b) ρ_{xx} vs H when the sample is uniformly magnetized. The field is applied along the [001] direction with current flowing parallel to the DWs at 10 K. The arrows indicate the field-sweeping direction. (c) MR of the DW at 10 K with the field applied along the [001] direction with current parallel to the DWs. All units are in $\mu\Omega$ cm.

between Figs. 3 and 4, respectively. Note that the direction of the domain walls is determined by the film structure and is parallel to the in-plane projection of the easy axis. Therefore, the measurements in the two figures are performed on different patterns (with perpendicular current paths) on the same film leading to the different zero resistivities.

We note that ρ_{xx}^{DWs} is field symmetric and does not change with field cycling, which indicates that the field has not induced DW motion and annihilation. Therefore, it is indeed possible to isolate the MR of the DW. In the following, we address two main features of $\rho_{\mathrm{DW}}^{\perp}$ and $\rho_{\mathrm{DW}}^{\parallel}$: the high-field negative MR and the low-field hysteretic behavior.

The low-field hysteretic behavior of $\rho_{\mathrm{DW}}^{\perp}$ and $\rho_{\mathrm{DW}}^{\parallel}$ indicates that the DWs can be in two states and that switching between them can be induced by applying a magnetic field perpendicularly to the DW plane. A possible difference between the two states can be the chirality of the DW. However, if chirality switching is induced by a field in the [001] direction, it implies that the magnetic moments in the DW have a component in the [001] direction, as well. This means that the DW cannot be a pure Bloch wall for which the magnetic moment rotates in the

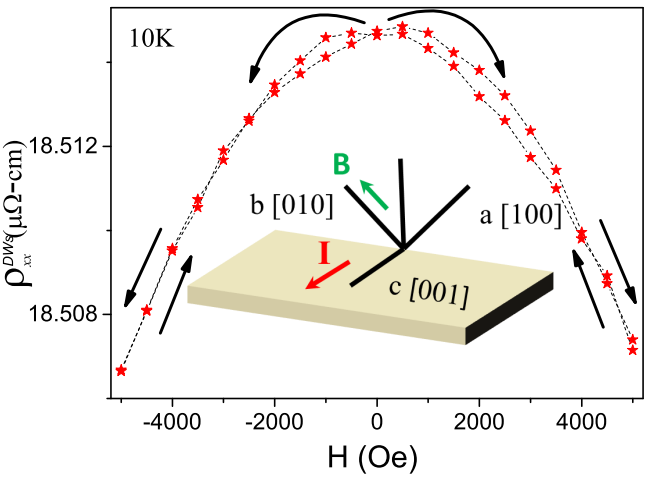

FIG. 5. ρ_{xx} vs H when the sample is in a domain state. The field is applied along the hard axis in the (001) plane. The arrows indicate the field-sweeping direction. Here, the current flows perpendicular to the DWs.

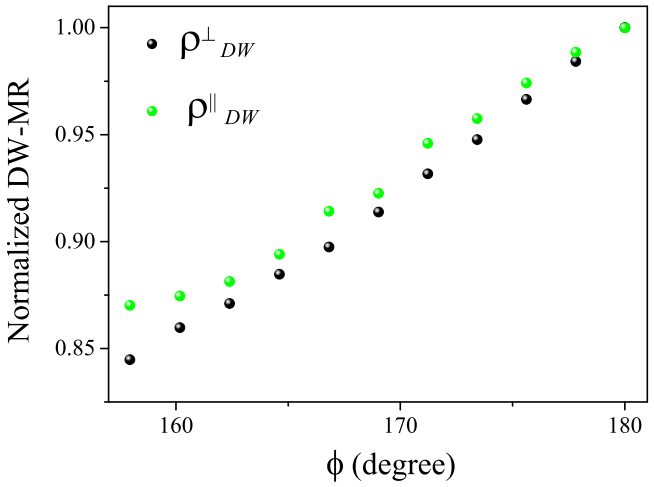

FIG. 6. The MR of the DWR normalized with DWR at zero field vs ϕ.

DW plane. If, on the other hand, the wall is a pure Néel wall then it would imply that the axis of rotation of the magnetic moments in the wall is in the wall plane, perpendicular to the easy axis. To explore this possibility, we measure $\rho^{\perp}_{\mathrm{DW}}$ in configuration 3 (see Fig. 5). The fact that $\rho^{\perp}_{\mathrm{DW}}$ is hysteretic at low fields clearly indicates that a pure Néel wall is also inconsistent with the results.

IV. DISCUSSION

We discuss potential mechanisms for the high-field negative MR of the DWR and the low-field hysteretic behavior and support our interpretation with numerical simulations.

At high fields, $\rho^{\perp}_{\mathrm{DW}}$ and $\rho^{\parallel}_{\mathrm{DW}}$ exhibit roughly linear negative MR. A possible source for this behavior is the decrease in the angle ϕ between the magnetization vectors in the neighboring domains. At zero applied field $\phi = \pi$ and clearly when ϕ goes to zero the DWR should vanish. At intermediate angles we may expect that the relative suppression of ϕ will be on the order of the suppression of the DWR. To test this scenario we show in Fig. 6 the DWR normalized by its zero-field value as a function of ϕ calculated according to the Stoner–Wohlfarth model [14], using an anisotropy field of 7 T. We note that the relative change of ∼3% in the normalized DWR corresponds with a change of ∼2.7% in ϕ, which appears to support this scenario.

We turn now to discuss the low-field hysteretic behavior of the DWR with the field applied along [001] and along the hard axis in the (001) plane. To explore this behavior, we have performed micromagnetic simulations with the MUMAX3 package [15]. The DW configuration is simulated on a 200×200 nm^2 region of thickness 20 nm. The cell size is $1 \times 1 \times 1$ nm^3. The uniaxial anisotropy direction lies in the (001) plane and tilts 30° from the film normal [13]. We take the magnetization to be $M_s = 0.21 \times 10^6$ A/m and uniaxial anisotropy $K_u = 1.2$ MJ/m^3 [13]. We applied a magnetic field along [001] and the hard axis in the (001) plane to simulate Néel and Bloch DW dynamics, respectively.

The numerical simulations indicate that the hysteresis is associated with DW-chirality reversal. Furthermore, when the

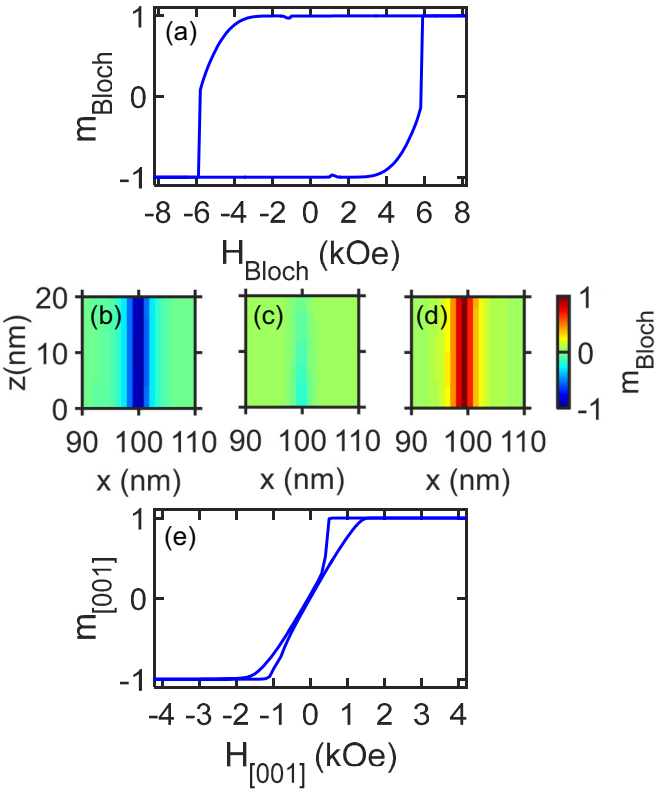

FIG. 7. (a) Magnetization component in the center of the domain wall along the hard axis in the (001) plane vs H along the same direction (b)–(d) Snapshot of the magnetic state inside the DW for H values of −6000, 5800, and 6000 Oe. (e) Magnetization component [001] in the center of domain wall vs H along [001].

field is applied in the [001] direction a Néel wall is stabilized whereas a Bloch wall is stabilized when the field is applied along the hard axis in the (001) plane.

Figure 7 shows some of the simulations results. In Fig. 7(a) a magnetic field is applied along the hard axis in the (001) plane, and it shows the magnetization component in the center of the domain wall in this direction. The relevant snapshot inside the DW denoting the magnetic state during the hysteresis is shown in Figs. 7(b)–7(e) with the associated color scale kept at the side of the respective images. At high fields we see a saturated uniform chiral state consistent with the field. Starting in a saturated state, if the field is reversed, there is a field range in which the initial DW chirality is maintained and only when the field exceeds a certain threshold does a Bloch line emerge at the DW edge and start propagating until a uniform chiral state with reversed chirality is reached [see Fig. 7(d)].

These observations are relevant for understanding the onset of the chirality reversal field as well as the irreversibility field as seen in Fig. 5 for configuration 3. The chirality reversal field and the irreversibility field are found to be 500 Oe and 4000 Oe, respectively, in the experiments, whereas our simulations show chirality reversal at 5800 Oe [see Fig. 7(c)] and irreversibility at 6000 Oe [see Fig. 7(d)]. The discrepancies in the values of the chirality reversal field can be attributed to the fact that DWs in the films experience pinning forces which are not considered in the simulations. The pinning hinders the movement of the Bloch line at a lower fields thus leading to the increase in

the chirality-reversal field in comparison with the simulation. Once a Bloch line emerges in the DW, the irreversibility field occurs at the same field range.

Figure 7(e) shows the results of simulations in which a magnetic field is applied along the [001] direction and the magnetization component in the center of the domain wall in this direction is plotted with the applied magnetic field. The hysteretic nature of the [001] component of the magnetization suggests that the Néel walls can also be realized in the system which can be stabilized by tuning the external applied field.

Commonly, transitions between Bloch and Néel walls are achieved by varying the thickness of the magnetic film [16–19], whereas we observe that both Bloch and Néel walls can be stabilized in the same film and this is observed for two different thicknesses (∼20 and ∼90 nm).

The ability to control the domain-wall type and chirality makes $SrRuO_3$ a particularly useful material system for studying the interaction of DWs with spin-orbit torques (SOTs). SOTs are interesting since there represent as yet unanswered fundamental questions related to the role played by the different responsible mechanisms. SOTs are also interesting because they emerge as effective tools for manipulating magnetic configurations on the nanometer scale and because they are expected to play a central role in future spintronics devices. Consequently, a comprehensive understanding of SOTs is important both for fundamental research and for applications. Two types of SOTs are predicted: a field-like torque and an antidamping-like torque whose effectiveness for a given configuration depends on the DW type (Bloch or Néel) and chirality. Thus, a system where the DW type and chirality can be tuned opens new ways to achieve a better understanding of SOTs.

To explore the possibility of studying the interaction between DWs and SOT, we will be investigating bilayer films of $SrRuO_3$ and a heavy metal (HM). In these films the structure of the wall (Bloch or Néel) and its chirality would be determined by applying a sufficiently large magnetic field in the appropriate direction. As the direction of the DWs is fixed relative to the substrate, we will fabricate samples with patterns rotated at different angles to each other. We will study the SOTs in three different states: (a) a fully magnetized state, (b) a stripe domain state, and (c) an individual DW state. For each state the current will be injected along opposite directions and with opposite polarities.

V. SUMMARY

Applying a magnetic field at directions perpendicular to the easy axis when $SrRuO_3$ is in a domain state affects the DWs without changing the domain structure. In the high-field regime we note negative MR of the DWR which can be correlated with the angular change between the neighboring domains. At low fields we note a hysteretic behavior, which indicates that either Bloch or Néel walls can be stabilized with a predetermined chirality at zero field by applying (and removing) a sufficiently large external magnetic field at appropriate directions perpendicular to the easy axis. The results open new opportunities for studying the effect of the structure and chirality of the DWs on the efficiency of spin-orbit and spin-transfer torques.

ACKNOWLEDGMENTS

L.K., A.D.K., and C.H.A. acknowledge support by the U.S.-Israel Binational Science Foundation (2012169). L.K. acknowledges support by the Israel Science Foundation founded by the Israel Academy of Sciences and Humanities (533/15). Research at NYU was supported by NSF-DMR-1610416. J.W.R. grew some of the samples used for this study at Stanford University in the laboratory of M.R. Beasley. F.J.W. and C.H.A. acknowledge support from the National Science Foundation under MRSEC DMR-1119826 (CRISP) and DMR-1309868.

[1] A. Hubert and R. Schafer, *Magnetic Domains: The Analysis of Magnetic Microstructures* (Springer, Berlin, 1998).
[2] J. Stohr and H. C. Siegmann, *Magnetism: From Fundamentals to Nanoscale Dynamics* (Springer, Berlin, 2007).
[3] L. Berger, Phys. Rev. B **54**, 9353 (1996).
[4] S. S. P. Parkin, M. Hayashi, and L. Thomas, Science **320**, 190 (2008).
[5] L. Thomas, R. Moriya, C. Rettner, and S. S. P. Parkin, Science **330**, 1810 (2010).
[6] L. Klein, J. S. Dodge, C. H. Ahn, J. W. Reiner, L. Mieville, T. H. Geballe, M. R. Beasley, and A. Kapitulnik, J. Phys.: Condens. Matter **8**, 10111 (1996).
[7] L. Klein, Y. Kats, A. F. Marshall, J. W. Reiner, T. H. Geballe, M. R. Beasley, and A. Kapitulnik, Phys. Rev. Lett. **84**, 6090 (2000).
[8] M. Feigenson, L. Klein, J. W. Reiner, and M. R. Beasley, Phys. Rev. B **67**, 134436 (2003).
[9] M. Feigenson, J. W. Reiner, and L. Klein, Phys. Rev. Lett. **98**, 247204 (2007).
[10] C. H. Ahn, R. H. Hammond, T. H. Geballe, M. R. Beasley, and J. M. Triscone, Appl. Phys. Lett. **70**, 206 (1997).
[11] Q. Gan, R. A. Rao, C. B. Eom, Appl. Phys. Lett. **70** 1962 (1997).
[12] G. Koster, L. Klein, W. Siemons, G. Rijnders, J. S. Dodge, C.-B. Eom, D. H. A. Blank, and M. R. Beasley, Rev. Mod. Phys. **84**, 253 (2012).
[13] Y. Kats, I. Genish, L. Klein, J. W. Reiner, and M. R. Beasley, Phys. Rev. B **71**, 100403(R) (2005).
[14] E. C. Stoner and E. P. Wohlfarth, Philos. Trans. R. Soc., A **240**, 599 (1948).
[15] A. Vansteenkiste, J. Leliaert, M. Dvornik, M. Helsen, F. G. Sanchez, and B. V. Waeyenberge, AIP Adv. **4**, 107133 (2014).
[16] E. J. Torok, A. L. Olson, and H. N. Oredson, J. Appl. Phys. **36**, 1394 (1966); T. Trunk, M. Redjdal, A. Kkay, M. F. Ruane, and F. B. Humphrey, *ibid.* **89**, 7606 (2001).
[17] M. Ziese, I. Vrejoiu, and D. Hesse, Appl. Phys. Lett. **97**, 052504 (2010).
[18] A. D. Kent, J. Yu, U. Ruediger, and S. S. P. Parkin, J. Phys.: Condens. Matter **13**, R461 (2001).
[19] C. L. S. Kantner, M. C. Langner, W. Siemons, J. L. Blok, G. Koster, A. J. H. M. Rijnders, R. Ramesh, and J. Orenstein, Phys. Rev. B **83**, 134432 (2011).